EUROSENSORS 2015

# Effect of stators geometry on the resonance sensitivity of capacitive MEMS

A. Frangi, G. Laghi[*], P. Minotti, G. Langfelder

*Politecnico di Milano, P.za Leonardo da Vinci 32, Milano 20133, Italy*

## Abstract

The work investigates alternative capacitive sensing topologies for microelectromechanical systems, that simultaneously enable large quasi-stationary sensitivity, comparable to parallel-plates configuration, and large quality (Q) factor. In agreement with the model predictions, about 3-fold larger Q factor and 2-fold larger resonant sensitivity are obtained on the optimized geometry.

*Keywords:* MEMS; inertial sensors; damping; capacitive sensing, stator optimization.

## 1. Introduction

In microelectromechanical systems (MEMS), capacitive sensing is commonly performed via either gap varying (parallel plates) or area-varying (comb-fingers) electrodes. In several MEMS resonators or resonant sensors, it would be beneficial to obtain both a large quality factor and a large quasi-stationary sensitivity, as the overall capacitive variation, signal output and phase noise at resonance improve with the product of both these terms. It is the case, for example, of gyroscopes drive loops [1], resonant accelerometers [2], and AM and FM resonant MEMS magnetometers [3-5]. Parallel-plate sensing shows large stationary sensitivity thanks to the inherently large capacitance variation per unit displacement *dC/dx*, yet it is characterized by poor Q factor due to squeezed film damping, that dominates in this kind of sensing geometry [6] at typical pressures of MEMS inertial sensors. On the other side, comb fingers show a high Q factor, thanks to the escape paths for the gas molecules provided by the geometry, but a lower sensitivity *dC/dx*.

————

* Corresponding author: Giacomo Laghi. Tel.: +39-022399-3744 *E-mail address:* giacomo.laghi@polimi.it

Alternative capacitive sensing geometries were investigated in previous work [7], with the purpose of improving the sensing performance.

This work continues and deepens the analysis through further geometrical refinements of the electrodes and through a direct comparison with a parallel plate configuration. Starting from the parallel plate case, suitable escapes for squeezed gas are gradually introduced, without significantly affecting the quasi-stationary capacitive sensitivity. The focus is on the free molecule-flow gas regime, representative of several MEMS sensors operating conditions.

A numerical model, which theoretically predicts the behavior of the designed devices in the mentioned pressure range, was developed and experimentally verified, showing an improvement both in sensitivity and Q, of a factor 2 and 3 respectively, for the optimized geometry with respect to the standard parallel-plates one.

## 2. Test devices and conditions

The test devices are fabricated using the ThELMA technology [8] (thick epitaxial layer for microactuators and accelerometers) from ST Microelectronics, which consists first in an epitaxial growth of a polycristalline Silicon layer. After deep reactive ion etching and dry hydrofluoric acid release, this layer becomes the 22-µm-thick structural layer of the MEMS devices. A thin underneath layer of polysilicon (650 nm) is also used to bring electrical signals from the structures to the external pads.

The four different test resonators designed for this work, shown in the top view of Fig. 1a, are formed by 3.4-µm-wide, 1050-µm-long clamped-clamped beams featuring a central suspended mass to set the first mode resonance frequency in the 15-20 kHz range, typical e.g. of consumer-grade MEMS gyroscopes.
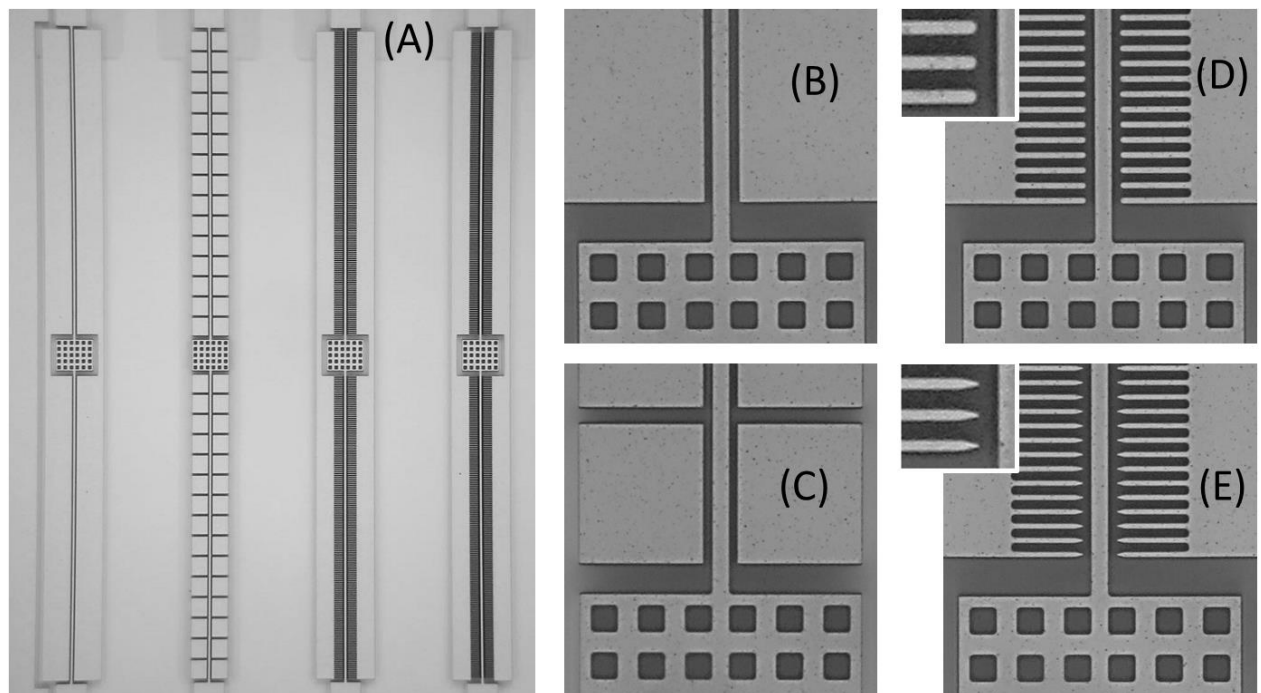


Fig. 1. Top-view (A) of the four resonators of this work, with details of the capacitive sensing electrodes geometries, gradually changing from the parallel-plate configuration (B) by adding escape routes for squeezed-film damping (C) with variable density (D) and refined tip geometry (E).

The devices lie all in the same package to guarantee identical pressure and as similar as possible etching conditions. The four identical beams are surrounded by different sensing geometries, gradually improving the performances in terms of Q-factor and quasi-stationary sensitivity of the whole device. Looking at Fig. 1, the four sensing electrode

designed geometries are shown: standard parallel-plates (B), holed stators (C) comb shaped stators (D) and arrow shaped stators (E). The difference between the (D) and (E) geometries can be better appreciated from the corresponding insets. All the electrodes have a 1.8-µm nominal gap distance from the suspended beam.

## 3. Numerical Model

The shown geometries represent a gradual optimization of the trade-off between (i) Q factor and (ii) stationary sensitivity: the former is studied through a custom boundary element model based on the theory of free-molecule flow [4,10], and Fig. 2 shows an example of the developed boundary mesh for the device E and of the corresponding calculated damping force field. The latter can be predicted with common finite element simulators.
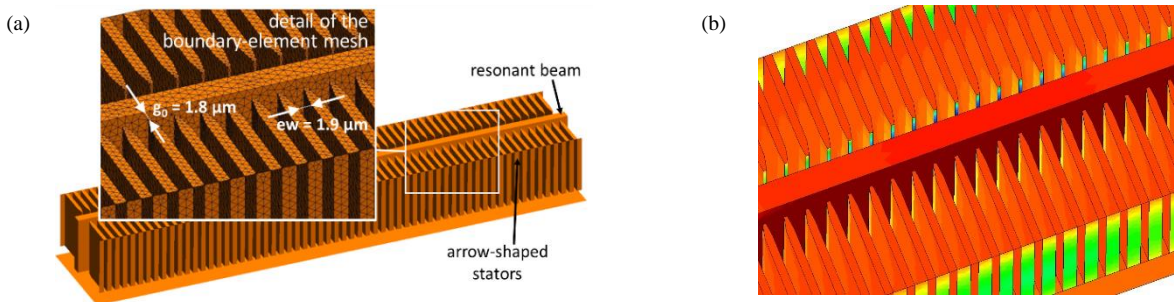


Fig. 2: (a) geometric model employed for the custom simulation of the dissipation coefficient in case E (arrow-shaped stators). The inset shows a detail of the used mesh with nominal geometrical parameters; (b) typical output of the numerical analysis: force field (in the direction orthogonal to the vibrating plate) exerted by the gas on the shuttle.

## 4. Experimental results

The devices, nominally packaged at a relatively low pressure (0.8 - 1 mbar), are then tested through a MEMS dedicated characterization platform from *ITmems s.r.l.* [9]. Two kinds of analyses are performed to extrapolate the characteristic parameters and compare the four devices. The first is a dynamic analysis, which is performed applying a square voltage wave to the one resonator port, while measuring the natural response of the device on the falling edge - when the voltage comes back to 0V - from the other electrode. The Q factor is then measured through a best-fitting procedure, both in the frequency (Fig. 3a) and in the time (Fig. 3b) domain. A 3-fold improvement for the arrow-shaped stator geometry with respect to the standard parallel plates is obtained.
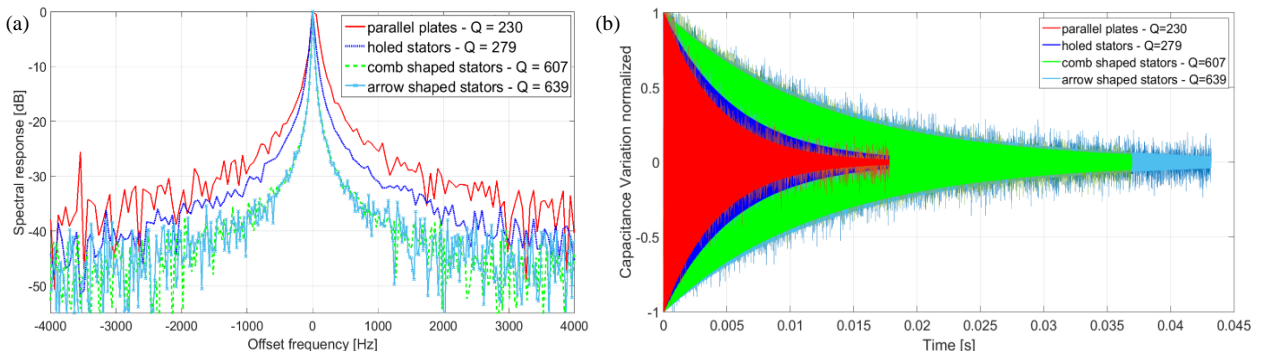


Fig. 3. Experimental measurements of (a) the spectral response, estimated through a ring-down technique and (b) the time-domain damping analysis for the devices of Fig. 1. The Q factor is obtained from a best-fitting procedure, cross-checked both on the spectral response and on the time-domain curve, showing a 3-fold ratio between parallel-plate and arrow-shaped stators.

The second analysis, shown in fig. 4a, is represented by the C-V curve, obtained applying a constant voltage at one electrode (used as drive), while measuring the capacitance value through the other port (used as sense). From this measurement, it is possible to extract a parameter (the square root of the parabolic coefficient, $\sqrt{C''}$) that is proportional to the quasi-stationary sensitivity of the device. Fig. 4b reports the product of this parameter, multiplied by the above measured quality factor, to obtain a figure of merit representative of sensitivity at resonance.
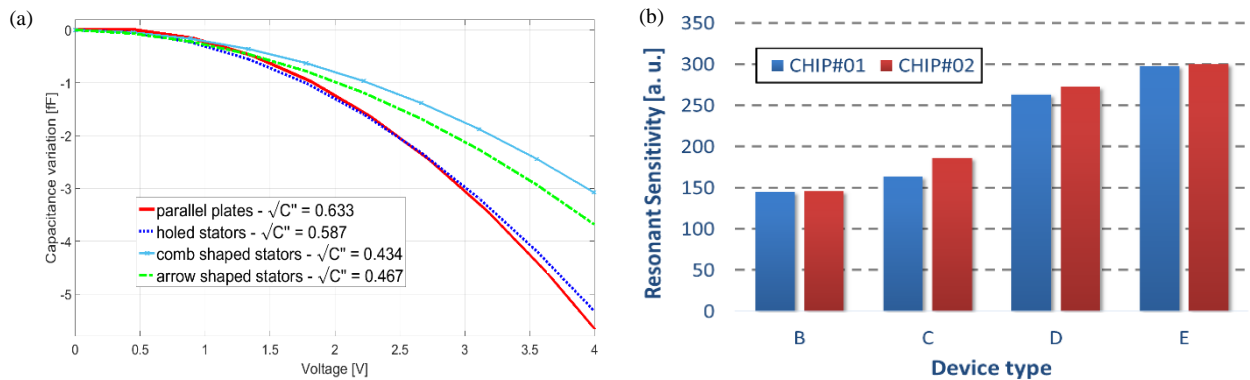


Fig. 4. (a) measurements of the quasi-stationary responses, through CV curves, for the four test structures of this work. The shown square root of the parabolic coefficient is directly related to the quasi-stationary sensitivity, shown in (b) the histogram form for two different chips. A 2-fold larger value is obtained for the optimized arrow-shaped case with respect to the standard parallel-plates configuration.

A more than 2-fold larger value of resonant sensitivity is obtained for the arrow-shaped stator with respect to the parallel-plate geometry, a result that overcomes by a factor 3 previous achievements presented in the literature [7]. For device E, at an assumed package pressure of 1mbar, the numerically estimated Q is 680, while the predicted differential capacitance variation $\Delta C/\Delta B$ per unit magnetic field is 9.01 aF/(µT mA)

### Acknowledgements

### References

[1] M.H. Kline et al., Quadrature FM gyroscope, Proc. IEEE MEMS 2013, Taipei, Taiwan, Jan 2013, pp.604-608
[2] G. Langfelder et al., Design criteria of low-power oscillators for consumer-grade MEMS resonant sensors, IEEE Transactions on Industrial Electronics, Vol. 61, N. 1, 2014, pp. 567-574.
[3] G. Langfelder et al., Off-Resonance Low-Pressure Operation of Lorentz Force MEMS Magnetometers, Industrial Electronics, IEEE Transactions on, vol. 61, no. 12, pp. 7124–7130, Dec 2014
[4] J. Kyynarainen et al., A 3D micromechanical compass, Sensors and ActuatorsA: Physical, vol. 142, no. 2, pp. 561–568, 2008
[5] M. Li et al., Extended Bandwidth Lorentz Force Magnetometer Based on Quadrature Frequency Modulation Microelectromechanical Systems, Journal of, 2014
[6] G. Langfelder et al., Z-Axis Magnetometers for MEMS Inertial Measurement Units Using an Industrial Process, IEEE Transactions on Industrial Electronics, vol. 60, n. 9, 3983–3990, Sep 2013
[7] A. Frangi et al., Optimization of Sensing Stators in Capacitive MEMS Operating at Resonance, Journal of Microelectromechanical Systems, in press, doi: 10.1109/JMEMS.2014.2381515.
[8] G. Langfelder et al., MEMS motion sensors based on the variations of the fringe capacitances, IEEE Sensors Journal, Vol. 11, n. 4, 2011.
[9] MEMS Characterization Platform, MCP-G, Product Data-Sheet, ITMEMS s.r.l., Milano, Italy, Accessed July 2015. [Online]. Available: http://www.itmems.it
[10] Frangi A., Ghisi A., Coronato L., On a deterministic approach for the evaluation of gas damping in inertial MEMS in the free-molecule regime, Sensor & Actuators, A 149, 21–28, 2009